Elastic Heterogeneity in Metallic Glasses

W. Dmowski,[1] T. Iwashita,[2] C.-P. Chuang,[1] J. Almer,[3] and T. Egami[1,2,4]

[1]*Department of Materials Science and Engineering, University of Tennessee, Knoxville, Tennessee 37996, USA*
[2]*Department of Physics and Astronomy, University of Tennessee, Knoxville, Tennessee 37996, USA*
[3]*Advanced Photon Source, Argonne National Laboratory, Argonne, Illinois 60439, USA*
[4]*Oak Ridge National Laboratory, Oak Ridge, Tennessee 37831, USA*

(Received 17 May 2010; published 11 November 2010)

When a stress is applied on a metallic glass it deforms following Hook's law. Therefore it may appear obvious that a metallic glass deforms elastically. Using x-ray diffraction and anisotropic pair-density function analysis we show that only about $\frac{3}{4}$ in volume fraction of metallic glasses deforms elastically, whereas the rest of the volume is anelastic and in the experimental time scale deform without resistance. We suggest that this anelastic portion represents residual liquidity in the glassy state. Many theories, such as the free-volume theory, assume the density of defects in the glassy state to be of the order of 1%, but this result shows that it is as much as a quarter.

DOI: 10.1103/PhysRevLett.105.205502 PACS numbers: 62.20.dj, 62.40.+i

Bulk metallic glasses are promising as structural material because of their extremely high strength [1,2]. Therefore it is important to understand the mechanism of deformation, whereas we are far from achieving this goal. In this Letter we show that even the elastic properties of metallic glasses are deeply misunderstood. Macroscopically metallic glasses appear to deform elastically, but at the atomic level elastic response is highly inhomogeneous, reflecting the intrinsic structural heterogeneity. For instance local atomic displacements are not collinear (nonaffine), and displacements are different from atom to atom [3]. Furthermore metallic glasses are viscoelastic, as other glasses [4–6], and a significant portion of the apparently elastic response could be due to anelasticity according to a simulation [7]. In this article we show that a significant fraction (as much as about a quarter) of the apparently elastic response of a metallic glass is indeed anelastic, through the analysis of x-ray diffraction results.

The lattice strains in crystalline materials can be measured directly by diffraction experiments, for instance, using x rays, electrons or neutrons. In glasses, which do not have periodicity in the atomic structure, it is not so obvious if the same can be done or not. Nevertheless, it has been claimed [8] that the local strain in metallic glasses can be measured using diffraction, by tracing shifts in the first peak in the structure function, $S(Q)$ where $Q = 4\pi \sin\theta/\lambda$ is the diffraction vector, θ diffraction angle and λ the wavelength of the probe, or the oscillations in the atomic pair-density function (PDF), which can be obtained by Fourier-transforming $S(Q)$

$$g(r) = 1 + \frac{1}{2\pi^2 r\rho_0}\int [S(Q) - 1]\sin QrQdQ \qquad (1)$$

where ρ_0 is the number density of atoms, with Q either parallel or perpendicular to the stress axis.

However, this equation is valid only when the system is isotropic [9]. For anisotropic bodies we have to expand the structure factor as well as PDF by the spherical harmonics $Y_\ell^m(\boldsymbol{x})$ [10],

$$g(\boldsymbol{r}) = \sum_{\ell,m} g_\ell^m(r) Y_\ell^m\left(\frac{\boldsymbol{r}}{r}\right), \qquad S(\boldsymbol{Q}) = \sum_{\ell,m} S_\ell^m(Q) Y_\ell^m\left(\frac{\boldsymbol{Q}}{Q}\right) \quad (2)$$

which are connected through the spherical Bessel transformation,

$$g_\ell^m(r) = \frac{(i)^\ell}{2\pi^2\rho_0}\int S_\ell^m(Q) J_\ell(Qr) Q^2 dQ, \qquad (3)$$

where $J_\ell(x)$ is the spherical Bessel function. Note that only for the isotropic component ($\ell = 0$), $J_0(x) = \sin x/x$ and Eq. (1) is recovered. For axial symmetry the terms with $\ell = 2$ and $m = 0$ have to be evaluated. Further details are given in Ref [11].

We carried out the x-ray diffraction measurements at the 1-ID/XOR beam line of the Advanced Photon Source, Argonne National Laboratory. The incident energy was tuned to 120 keV ($\lambda = 0.10332$ Å). The beam size was set to 0.2 mm × 0.2 mm. The MAR345 area detector, placed 40 cm behind the sample, was used in collecting diffracted x rays. As a sample we used Vit-105 metallic glasses with the composition of $Zr_{52.5}Cu_{17.9}Ni_{14.6}Al_{10}Ti_5$. Samples were prepared by a melt casting into 1.5 mm thick plates. The dog-bone shapes, with the central part being 9.6 mm long, were cut using electric discharge machining (EDM) . The samples were polished to the final thickness of 0.67 mm and the width of 2 mm. The sample was placed in a tensile grip in a MTS load frame Model 858. Sample grips were encircled in an infrared heater with a front opening of ±30 degrees. The design of the heater permitted unobstructed scattering from the sample. The external stress was varied from 0 to 1.2 GPa with a 0.2 step. After

reaching 1.2 GPa the temperature was increased to 300 °C and held for 30 min to induce creep deformation. After 30 min the sample reached the steady state rate. Then the sample was cooled and after reaching room temperature the external load was removed. The elongation after reaching room temperature was 2%. At each step x-ray scattering was collected for approximately 1 h. For each measurement step frames were summed and the background due to dark current was subtracted. Data were then normalized by the incident beam monitor, and the expansion into spherical harmonics was performed to determine the anisotropic components of the $S(\boldsymbol{Q})$ and $g(\boldsymbol{r})$.

We found that the isotropic ($\ell = 0$) component of $S(\boldsymbol{Q})$, $S_0^0(Q)$, shows very small changes with the applied stress, but, the elliptical ($\ell = 2$) component, $S_2^0(Q)$, shows significant changes as is shown in the Fig. 1. The amplitude of $S_2^0(Q)$ is roughly proportional to the stress, whereas the shape is almost independent of the stress. The elliptical ($\ell = 2$) component of the PDF, $g_{2,\mathrm{obs}}^0(r)$, was obtained by the spherical Bessel transformation, Eq. (3), and is shown in Fig. 2. The $g_{2,\mathrm{obs}}^0(r)$ is roughly proportional to the stress in amplitude, while the shape remains almost unchanged, as expected from the behavior of $S_2^0(Q)$.

It can be shown that for axial elongation along z, the elliptical PDF due to affine deformation, $g_{2,\mathrm{aff}}^0(r)$, can be expressed in terms of the derivative of the isotropic PDF, $g_0^0(r)$ [10];

$$g_{2,\mathrm{aff}}^0(r) = \varepsilon_{zz,\mathrm{aff}} \bar{g}_{2,\mathrm{aff}}^0(r) = -\varepsilon_{zz,\mathrm{aff}} \left(\frac{1}{5}\right)^{1/2} \frac{2(1+\nu)}{3} r \frac{d}{dr} g_0^0(r) \quad (4)$$

where ν is the Poisson's ratio. Indeed the experimentally observed $r g_{2,\mathrm{obs}}^0(r)$ is close to the derivative as shown in Fig. 3, particularly at large distances. We determined the amplitude of the apparent elastic strain, $\varepsilon_{\mathrm{app}}$, by matching the experimental $r g_{2,\mathrm{obs}}^0(r)$ to $r g_{2,\mathrm{aff}}^0(r)$ over the range of r between 6.6 and 25 Å, using the experimental value of $\nu(= 0.38)$ [12]; $\varepsilon_{\mathrm{app}} = \varepsilon_{zz,\mathrm{aff}}$ over this range. The apparent Young's modulus, $\sigma/\varepsilon_{\mathrm{app}}$, is 94.5 GPa, close to the value determined by ultrasound resonance method, 89 GPa [12]. Published results of the effective Young's modulus determined by diffraction experiments are close to, but slightly higher than those determined by ultrasound measurements [13].

However, Fig. 3 shows small but significant differences between the observed $g_2^0(r)$ and $g_{2,\mathrm{aff}}^0(r)$ below 6.6 Å. These differences could be caused by the anelastic events. Indeed earlier studies found that the apparent strain determined by

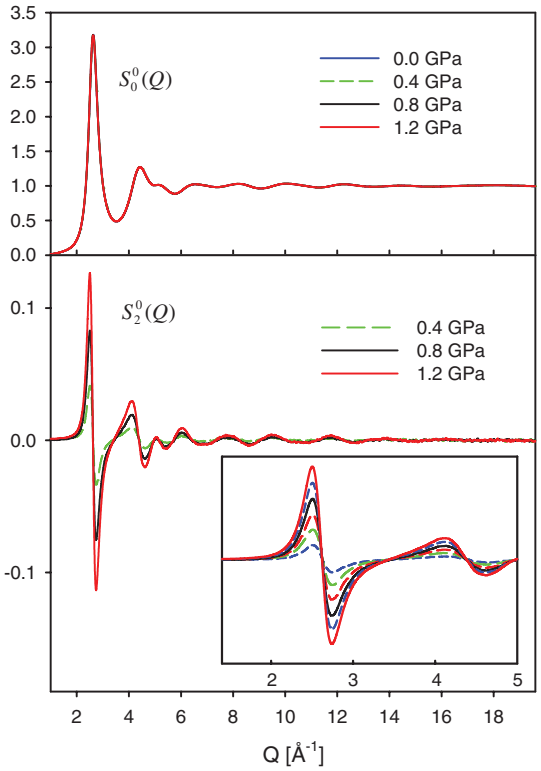

FIG. 1 (color). The isotropic part of the structure function, $S_0^0(Q)$, (above), and the changes in the $\ell = 2$ component of the structure factor, $S_2^0(Q)$ (below). For clarity only three stress levels are shown. The changes appear linear with the stress. The $S_2^0(Q)$ is also shown up to 5 Å in the inset with a stress step of 0.2, from 0.2 to 1.2 GPa.

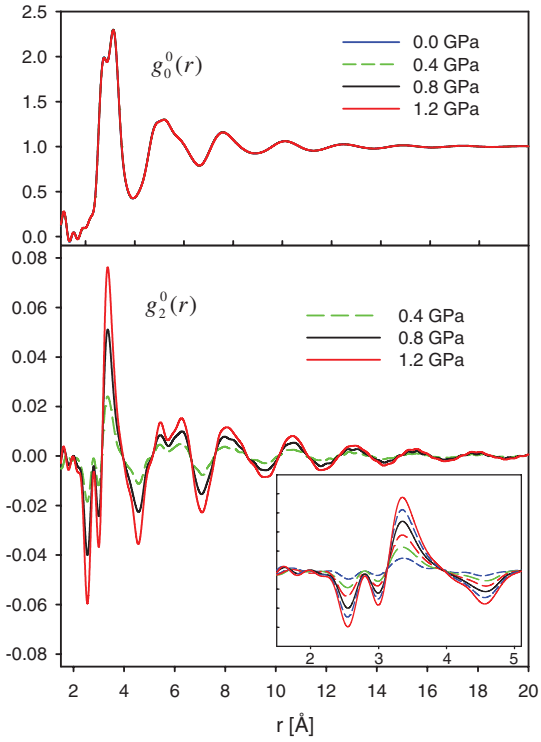

FIG. 2 (color). The isotropic part of the PDF, $g_0^0(r)$, (above), and the $\ell = 2$ component of the PDF, $g_2^0(r)$ (below), for different applied external loads. For clarity only three stress levels are shown. The $g_2^0(r)$ is also shown up to 5 Å in the inset with a stress step of 0.2, from 0.2 to 1.2 GPa. The amplitude of the anisotropic term is roughly proportional to the stress, whereas the shape remains largely unchanged.

the PDF analysis was not homogeneous, but was dependent on the atomic distance, r [8,14–17]. This has been suggested to be the effect of anelasticity [14]. However, in the earlier studies the elastic and anelastic contributions have not been quantitatively separated. An additional technical complication is that in most papers the strain was assessed from the isotropic PDF, $g(r)$, derived by Eq. (3).

When a stress is applied to a viscoelastic material the strain response is given by;

$$\varepsilon(\tau_{\mathrm{exp}}) = \varepsilon_{\mathrm{el}} + \int_0^{\infty} \varepsilon_{\mathrm{anel}}(\tau)[1 - e^{-\tau_{\mathrm{exp}}/\tau}]d\tau \qquad (5)$$

where $\varepsilon_{\mathrm{el}}$ is the elastic strain, τ_{exp} is the experimental time scale, for instance the inverse of the strain rate, τ is the relaxation time and $\varepsilon_{\mathrm{anel}}(\tau)d\tau$ is the anelastic strain with the relaxation time between τ and $\tau + d\tau$. By approximating the exponential function by a step function we obtain,

$$\varepsilon(\tau_{\mathrm{exp}}) \approx \varepsilon_{\mathrm{el}} + \int_0^{\tau_{\mathrm{exp}}} \varepsilon_{\mathrm{anel}}(\tau)d\tau. \qquad (6)$$

Thus all the viscoelastic responses with the response time shorter than the experimental time scale are included in the apparent elastic strain. In order to evaluate the anisotropic PDF due to the anelastic strain, we studied the sample which was creep deformed as described above, at the stress of 1.2 GPa and $T = 573$ K for 30 min., to obtain the $\ell = 2$ PDF, $g^0_{2,\mathrm{anel}}(r)$. As was found previously [10,18] and is shown in Fig. 4, $g^0_{2,\mathrm{anel}}(r)$ is similar to $g^0_{2,\mathrm{aff}}(r)$ at large distances. By comparing $g^0_{2,\mathrm{anel}}(r)$ to $g^0_{2,\mathrm{aff}}(r)$ at large distances we determined the anelastic creep strain for this particular experiment, $\varepsilon_{\mathrm{creep}}$, and obtained $\bar{g}^0_{2,\mathrm{anel}}(r)$ by normalizing $g^0_{2,\mathrm{anel}}(r)$ to the anelastic creep strain of unity. We found that the deviations of the anelastic PDF, $g^0_{2,\mathrm{anel}}(r)$, from the affine PDF, $g^0_{2,\mathrm{aff}}(r)$, are very similar to those for the tensile strain experiment after appropriate scaling. This similarity indicates that the local structural changes due to anelastic strain induced by the apparently elastic deformation are very similar to those due to the anelastic creep deformation, in spite of the differences in time scale and temperature. As will be discussed elsewhere the $\ell = 2$ PDF due to the anelastic effect is independent of the stress level except for the amplitude, and when normalized by the strain results in the identical $\bar{g}^0_{2,\mathrm{anel}}(r)$.

Therefore, the total PDF should be fit by

$$g^0_{2,\mathrm{total}}(r) = \varepsilon_{zz,\mathrm{anel}}\bar{g}^0_{2,\mathrm{anel}}(r) + (\varepsilon_{\mathrm{app}} - \varepsilon_{zz,\mathrm{anel}})\bar{g}^0_{2,\mathrm{aff}}(r), \quad (7)$$

where $\varepsilon_{zz,\mathrm{anel}}$ is the anelastic strain, and $\varepsilon_{zz,\mathrm{aff}} = \varepsilon_{\mathrm{app}} - \varepsilon_{zz,\mathrm{anel}}$ is the affine (elastic) strain. Figure 5 compares the observed $g^0_{2,\mathrm{obs}}(r)$ with $g^0_{2,\mathrm{total}}(r)$ at $\sigma = 1.2$ GPa. Except for small differences which are most likely due to the mismatch of resolution and noise, agreement is excellent, confirming that the strain in this metallic glass includes both the anelastic as well as affine components. The fraction of the affine strain to the total strain, $z = \varepsilon_{zz,\mathrm{aff}}/\varepsilon_{\mathrm{app}}$, is plotted as a function of the applied stress, σ, in the inset of Fig. 5. The value of z is nearly constant over this range of stress, and in average 24% of the total strain is anelastic. This result is in excellent agreement with the simulation that suggested that about 20% of the apparent elastic strain is actually an anelastic strain [7]. Many theories, such as

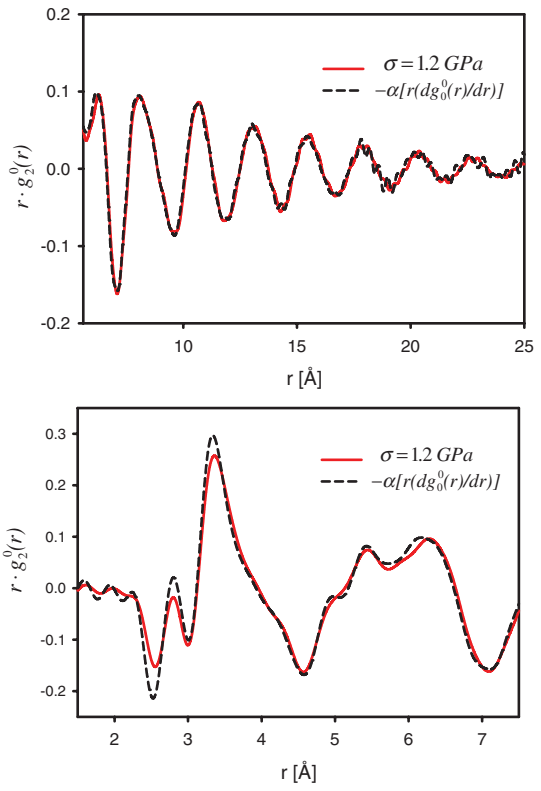

FIG. 3 (color). The $\ell = 2$ component of the PDF, $g^0_2(r)$, at the applied stress of 1.2 GPa (red solid line), compared to the PDF for affine deformation (black dashed line). Here we show $rg^0_2(r)$ in order to emphasize oscillations at large r. The fit is very good beyond 6.6 Å but obvious deviations are seen in the first atomic shell up to 4 Å.

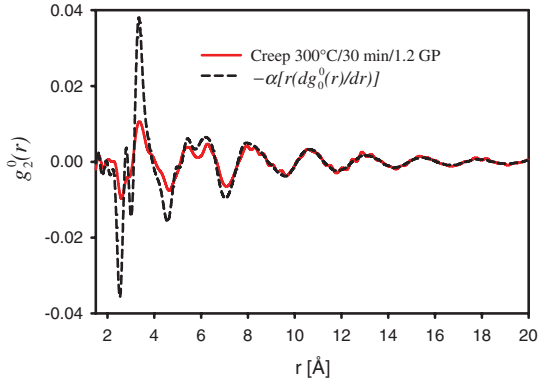

FIG. 4 (color). The $\ell = 2$ component of the PDF, $g^0_2(r)$, after creep at 574 K for 30 min with the applied load of 1.2 GPa. The dashed line shows the PDF expected for affine deformation, which is fitted to the data at large distances. The anelastic strain determined by the fit is 0.4%, whereas the total creep strain is 2%. The difference, 1.6%, is the plastic creep strain.

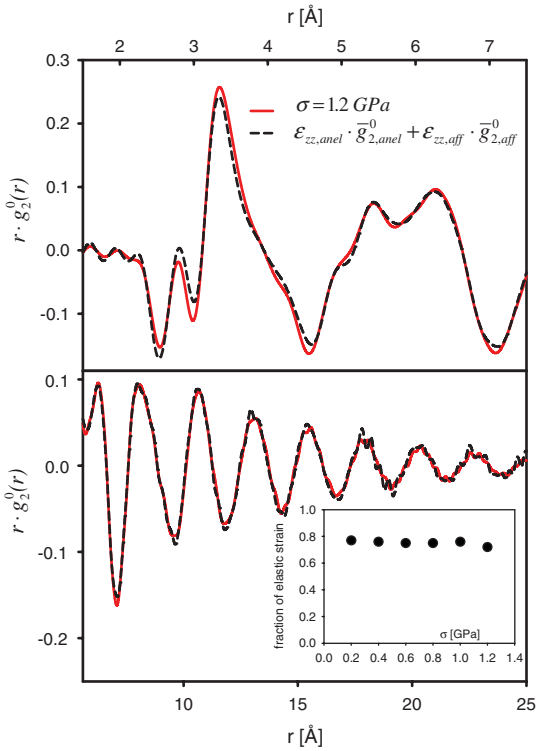

FIG. 5 (color). The $\ell = 2$ component of the PDF, $g^0_2(r)$, at 1.2 GPa, fitted to the combined PDF for affine and creep (anelastic) deformation, Eq. (7). The fit shows marked improvement over the one in Fig. 3 [11]. The inset shows the fraction of elastic strain compared to the total apparent strain. It appears constant of applied external stress up to 1 GPa, and on average it is about 76%. The rest, 24%, is the anelastic strain.

the free-volume theory, assume that the defect level is of the order of 1% [19], whereas the defect density suggested by the present study is higher by an order of magnitude. On the other hand this value agrees very well with the fraction of the frozen liquidlike atoms, 24.3%, in the theory of the glass transition in metallic glasses [20]. This point is important, and will be discussed separately elsewhere.

The analysis above suggests that the applied load is supported by only 76% of the body, and the rest, the anelastic sites, offer no resistance to load at the time scale of the experiment. Thus we can evaluate the true elastic constant of the elastic portion, $E_{\rm el} = \sigma/\varepsilon_{zz,\rm aff} = 124$ GPa. It has been known that the value of the shear modulus of a metallic glass is lower by 20%–30% than calculated for affine deformation [3,7] and the values for crystalline solids of the same composition [21]. The difference has been attributed to the noncollinear effect [3] and anelasticity [7]. Because the Young's modulus, E, is closely related to the shear modulus, G, ($E = G\frac{9}{3+G/B}$, B is the bulk modulus), the present result confirms that the apparent softening of the shear modulus occurs because about a quarter in volume fraction of a metallic glass is anelastic, and does not offer shear rigidity at the experimental time scale.

In conclusion, we have shown through x-ray scattering and the anisotropic PDF analysis that about a quarter of the volume of a metallic glass is occupied by anelastic sites, which are soft and bear no static shear load. Consequently the shear modulus of a metallic glass is lowered by a quarter compared to the instantaneous value. Just as other glasses, metallic glasses are fundamentally viscoelastic, and the volume fraction of the viscous sites is as much as a quarter, not of the order of 1% as in many theories. This point has to be fully taken into account in the application of metallic glasses, particularly as structural materials.

We acknowledge Professor P. K. Liaw for the use of his laboratory to prepare the samples. This work was supported by the Division of Materials Science and Engineering, Office of Basic Energy Sciences, Department of Energy, through Contract No. DE-AC05-00OR-22725. Use of the Advanced Photon Source is supported by the U.S. Department of Energy (DOE), Office of Science, under Contract No. DE-AC02-06CH11357.

[1] A. L. Greer, Science **267**, 1947 (1995).
[2] M. F. Ashby and A. L. Greer, Scr. Mater. **54**, 321 (2006).
[3] D. Waire, M. F. Ashby, J. Logan, and J. Weis, Acta Metall. **19**, 779 (1971).
[4] H.-S. Chen, H. J. Leamy, and J. Barmatz, J. Non-Cryst. Solids **5**, 444 (1971).
[5] N. Morito and T. Egami, Acta Metall. **32**, 603 (1984).
[6] Z. F. Zhao, P. Wen, C. H. Shek, and W. H. Wang, Phys. Rev. B **75**, 174201 (2007).
[7] Y. Suzuki and T. Egami, J. Non-Cryst. Solids **75**, 361 (1985).
[8] H. F. Paulsen, J. A. Wert, J. Neuefeind, V. Honkimaki, and M. Daymond, Nature Mater. **4**, 33 (2005).
[9] T. Egami and S. J. L. Billinge, *Underneath the Bragg Peaks: Structural Analysis of Complex Materials* (Pergamon Press, Elsevier Ltd., Oxford, 2003).
[10] Y. Suzuki, J. Haimovich, and T. Egami, Phys. Rev. B **35**, 2162 (1987).
[11] See supplementary material at http://link.aps.org/supplemental/10.1103/PhysRevLett.105.205502.
[12] Z. Zhang, V. Keppens, P. K. Liaw, Y. Tokoyama, and A. Inoue, J. Mater. Res. **22**, 364 (2007).
[13] M. Stoica, J. Das, J. Bednarcik, G. Wang, G. Vaughan, W. H. Wang, and J. Eckert, J. Met. **2010**, 76 (2010).
[14] T. C. Hufnagel, R. T. Ott, and J. Almer, Phys. Rev. B **73**, 064204 (2006).
[15] X. D. Wang, J. Bednarcik, K. Saksl, H. Franz, Q. P. Cao, and J. Z. Jiang, Appl. Phys. Lett. **91**, 081913 (2007).
[16] M. Stoica, J. Das, J. Bednarcik, H. Franz, N. Mattern, W. H. Wang, and J. Eckert, J. Appl. Phys. **104**, 013522 (2008).
[17] N. Mattern, J. Bednarcik, S. Pauly, G. Wang, J. Das, and J. Eckert, Acta Mater. **57**, 4133 (2009).
[18] W. Dmowski and T. Egami, J. Mater. Res. **22**, 412 (2007).
[19] M. H. Cohen and D. Turnbull, J. Chem. Phys. **31**, 1164 (1959).
[20] T. Egami, S. J. Poon, Z. Zhang, and V. Keppens, Phys. Rev. B **76**, 024203 (2007).
[21] L. A. Davis, in *Rapidly Quenched Metals* (MIT Press, Cambridge, MA, 1976), p. 369.